Biologically-Inspired Bodies Under Surface Waves—Part 2: Theoretical Control of Maneuvering

Promode R. Bandyopadhyay
Naval Undersea Warfare Center,
Newport, RI 02841
Fellow ASME

Sahjendra N. Singh
Professor. ECE Department.

Francis Chockalingam
Graduate Student. ECE Department.

University of Nevada,
Las Vegas, NV

The theoretical control of low-speed maneuvering of small underwater vehicles in the dive plane using dorsal and caudal fin-based control surfaces is considered. The two dorsal fins are long and are actually mounted in the horizontal plane. The caudal fin is also horizontal and is akin to the fluke of a whale. Dorsal-like fins mounted on a flow aligned vehicle produce a normal force when they are cambered. Using such a device, depth control can be accomplished. A flapping foil device mounted at the end of the tailcone of the vehicle produces vehicle motion that is somewhat similar to the motion produced by the caudal fins of fish. The moment produced by the flapping foils is used here for pitch angle control. A continuous adaptive sliding mode control law is derived for depth control via the dorsal fins in the presence of surface waves. The flapping foils have periodic motion and they can produce only periodic forces. A discrete adaptive predictive control law is designed for varying the maximum tip excursion of the foils in each cycle for the pitch angle control and for the attenuation of disturbance caused by waves. Strouhal number of the foils is the key control variable. The derivation of control laws requires only imprecise knowledge of the hydrodynamic parameters and large uncertainty in system parameters is allowed. In the closed-loop system, depth trajectory tracking and pitch angle control are accomplished using caudal and dorsal fin-based control surfaces in the presence of system parameter uncertainty and surface waves. A control law for the trajectory control of depth and regulation of the pitch angle is also presented, which uses only the dorsal fins and simulation results are presented to show the controller performance.

Introduction

Biologically inspired maneuvering of man-made under water vehicles has the potential of being agile and quiet. The dorsal and caudal fins give a fish a remarkable ability for swift and complex maneuvers (Wu et al., 1975 and Azuma, 1992). Here, we examine their potential for maneuvering small agile vehicles at low speeds. Studies have been carried out on fish morphology, locomotion, and the application of biologically-inspired control surfaces to rigid cylindrical bodies (Bandyopadhyay, 1996; Bandyopadhyay and Donnelly, 1997; Bandyopadhyay et al., 1997 and Part 1 of this paper). Related research to produce propulsive and lifting forces using flapping foil devices has been conducted by several authors (Chopra, 1977; Bainbridge, 1963; Gopalkrishnan et al., 1994; Triantafyllou et al., 1993; Hall and Hall, 1996; Triantafyllou et al., 1991). However, as yet, control systems synthesis using caudal and dorsal fins has not been accomplished.

The contribution of the present research lies in the design of control systems for low-speed maneuvering of small undersea vehicles using dorsal- and caudal-like fins (Fig. 1). A hydrodynamic control scheme is developed so that the vehicle tracks a precise depth versus time trajectory. It is assumed that the hydrodynamic parameters of the vehicle are imprecisely known and surface wave-induced forces are constantly acting on the vehicle. Although the design approach can be extended to yaw control, in this study, only control in the dive plane is considered. Using the dorsal fin, a normal force is produced for depth control and flapping foils produce pitching moment for pitch angle regulation. For simplicity, it is assumed that the vehicle is equipped with a control mechanism that causes the vehicle to move forward with a uniform velocity. For the depth trajectory control, an adaptive sliding mode control law (Slotine and Li, 1991; Utkin, 1978; and Narendra and Annaswamy, 1989) is designed for the continuous cambering of the dorsal fins in the presence of seawaves. The sliding mode control law is nonlinear and discontinuous in the state space and has an excellent insensitivity property with respect to disturbances and parameter variations.

The hydrodynamics of flapping foils is rather complex. Although design based on the continuous control of the angular velocity of the caudal fins is more efficient, forces and moments produced by the caudal-like fins as functions of angular position and velocity are not well-understood. This study is limited to a periodic (sinusoidal) actuation of caudal fins. It is assumed that the foils have identical periods of oscillation that do not necessarily coincide with the period of the seawave. The amplitude and phase of force and moment acting on the vehicle caused by the disturbing wave are assumed to be unknown. Assuming that the vehicle pitch angle deviation is small, a linear discrete adaptive predictive control system (Goodwin and Sin 1984) is designed for the pitch angle control. The maximum travel of the tips of the foils is adjusted periodically at the completion of the cycle. Interestingly, for the design of the pitch controller, it is seen that Strouhal numbers, which characterize the moment produced by the foils (caudal fins), are key control variables. In the closed-loop system using the dorsal and caudal fin controllers, depth control and pitch angle regulation in the dive plane are accomplished. Furthermore, a control system is designed for the control of depth and regulation of pitch angle using only dorsal fins and simulation results are presented.

Contributed by the Fluids Engineering Division for publication in the JOURNAL OF FLUIDS ENGINEERING. Manuscript received by the Fluids Engineering Division November 3, 1997; revised manuscript received December 4, 1998. Associate Technical Editor: M. Triantafyllou.

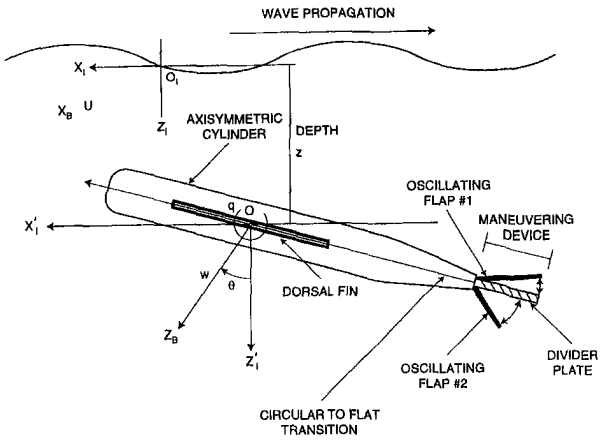

where:

$X_I - Z_I$ = Inertial Coordinate System (Origin at the Calm Surface).
$X_I' - Z_I'$ = Translation of Inertial Frame (Origin at Geometrical Center).
$X_B - Z_B$ = Body Fixed Coordinate System.

(Note that the long dorsal fins are actually mounted in the horizontal plane. The caudal fins are also mounted in the horizontal plane and are akin to flukes in whales.)

Fig. 1 Schematic of the maneuvering devices (Dorsal and Caudal Fins) and axisymmetric cylinder. Dorsal fin is shown uncambered.

Mathematical Model of Dive Plane Motion

Consider the vehicle motion in the dive (vertical) plane (Fig. 1). The heave and pitch equations of motion are described by coupled nonlinear differential equations. In a moving coordinate frame fixed at the vehicle's geometrical center, the dimensionless equations of motion for a neutrally buoyant vehicle are given by Papoulias and Papadimitriou (1995); Healy and Lienard (1993); and Smith et al. (1978)

$$m(\dot{w} - uq - z_G q^2 - x_G \dot{q}) = z_{\dot{q}}\dot{q} + z_{\dot{w}}\dot{w} + z_q q + z_w w - C_D \int_{\text{tail}}^{\text{nose}} b(x)(w - xq)|w - xq|dx + z_\delta \delta + f_p + f_d,$$

$$I_y \dot{q} + mz_G(\dot{u} + wq) - mx_G(\dot{w} - uq) = M_{\dot{q}}\dot{q} + M_{\dot{w}}\dot{w} + M_q q + M_w w + C_D \int_{\text{tail}}^{\text{nose}} xb(x)(w - xq)|w - xq|dx - x_{GB}W \cos\theta - z_{GB}W \sin\theta + m_p + m_d, \quad (1)$$

where $\dot{\theta} = q$, $\dot{z} = -u \sin\theta + w \cos\theta + \dot{z}_f$, $x_{GB} = x_G - x_B$, $z_{GB} = z_G - z_B$, δ is the camber of the dorsal fins, $m_p = m_{p1} + m_{p2}$, m_{pi} is the moment produced by the ith foil, f_p is the net normal force produced by the flapping foils, $\dot{z}_f$ is the velocity of the fluid, and m_d and f_d are the force and moment acting on the vehicle caused by the surface wave. (Camber is the maximum cross-stream deflection of the dorsal fin). Here it is assumed that the forward speed is held steady ($u = U$) by a control mechanism. These nondimensionalized equations of motion (Eq. (1)) are obtained by dividing the original force and moment equations by $\frac{1}{2}\rho L^2 V^2$ and $\frac{1}{2}\rho L^3 V^2$ where L and $V = U$ are the reference values for length and velocity, and the time is scaled by (U/L). Thus z_δ, f_p, and m_p are the hydrodynamic coefficients of the vertical force and the pitching moment from the control fins.

In Part 1, Bandyopadhyay et al. (1998) have experimentally measured the forces and moments acting on winged bodies submerged in proximity of surface waves. The disturbance force and moment caused by surface waves are periodic, which can be

Nomenclature

A_i, A_2 = maximum cross-stream travel of a flap tip
A_p, b_1, A_c, B_c, D_c = system matrices
a_i, b_{ii} = system parameters
$u = U$, w = vehicle's forward and normal velocity
q = pitch rate
θ = pitch angle
z = depth
δ = camber
$Z_{\dot{q}}$, $Z_{\dot{w}}$, Z_q, Z_w, Z_δ = coefficients used in representing normal force
$M_{\dot{q}}$, $M_{\dot{w}}$, M_q, M_w = coefficients used in representing moment
x_B, z_B = coordinates of CB
x_g, z_g = coordinates of CG
C_d = coefficient used in crossflow integration
m, W = mass, weight of vehicle
m_{p1}, m_{p2}, m_p = moments produced by caudal fins
m_d, f_d = moment and force due to surface wave
I_y = moment of inertia
ω_f, ω_o = frequencies of oscillation of foils and of surface wave
α_1, α_2, α_o = phase angles
F_{io}, F_{ij}, M_{io}, M_{ij} = flapping foil force and moment terms
S_{t1}, S_{t2} = Strouhal numbers of foils
$U_c = (\delta, f_p, m_p)^T$ = control vector
$\xi = (z, w, q, \theta)^T$ = state vector
$y_o = z$ = output variable to be controlled
y_r = reference depth trajectory
ζ_r, ω_r = command generator parameters
z^* = target depth
S = switching surface
$e = (y_o - y_r)$ = depth tracking error
λ = switching surface parameter
α, $\Delta\alpha$ = known and uncertain functions
F_{d1}, F_{d2} = amplitudes of sinusoidal force components due to surface wave
$\hat{F}_{d1}$, $\hat{F}_{d2}$, $\hat{\eta}$ = estimates of parameters in control law
L_1, L_2, L_3 = weighting parameters in the Lyapunov function
V_o = Lyapunov function
K, μ = gain, feedback parameter used in sliding mode control law
$e = (z - y_o)$ = tracking error
θ^*, q^*, ω^* = equilibrium values
T_p = period
q_a = advance operator
a_{cij}, B_{cj}, a_{fi}, B_{fi} = elements used in discrete-time representation of dynamics
$\tilde{\theta}$ = pitch angle error
J = performance index
ν, β = polynomials used for predicting pitch angle
ν_l, β_i = coefficients of polynomials
$\hat{\nu}$, $\hat{\beta}$ = estimated polynomials
$\hat{\nu}_i$, $\hat{\beta}_i$ = estimates of ν_l, β_i
ψ, $\phi(k)$ = regressor vectors
p_o = parameter vector

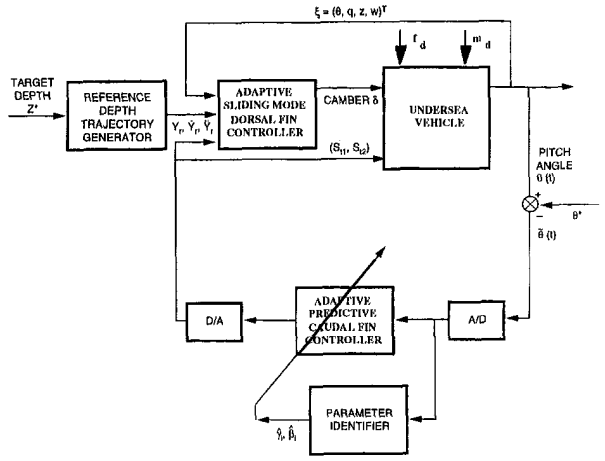

where

Z^* = **Target Depth,**
θ = **Pitch Angle,**
θ^* = **Equilibrium Pitch Angle,**
S_{t1}, S_{t2} = **Strouhal Numbers of Foils,**
A_1, A_2 = **Maximum Travel of Foils,**
δ = **Camber of Dorsal Fins.**

Fig. 2 Closed-loop system (Including the Caudal and Dorsal Fin Controllers)

expressed by a Fourier series. For simplicity in presentation, consider that f_d and m_d are well approximated by their fundamental components and are given by

$$f_d = F_d \cos(\omega_o t + \alpha_o)$$
$$m_d = M_d \cos(\omega_o t + \hat{\alpha}_o), \tag{2}$$

where ω_o is the fundamental frequency of the surface wave, F_d and M_d are amplitudes, and α_o and $\hat{\alpha}_o$ are the phase angles.

The dorsal fin produces a normal force ($z_\delta \delta$) proportional to the camber δ of the fins and can be continuously varied for the purpose of control. The forces and moments produced by the flapping foils (caudal fins) are quite complex and depend on motion pattern (clapping and waving) as well as on the frequency of oscillation, maximum flapping angles, axis about which foils oscillate, and the speed U. The motions of the foil pair in the tail are called clapping and waving, because of the patterns they mimic; in the former, the flaps are out of phase while they are in phase in the latter. The choice of flapping parameters and the mode of oscillation can produce a variety of control forces and moments. Based on the experimental results and analysis, it had been shown by Bandyopadhyay and coworkers (Bandyopadhyay, 1996; Bandyopadhyay and Donnelly, 1997; and Bandyopadhyay et al., 1997) that flapping foils produce periodic forces whose period is equal to the period of flapping. Therefore, their periodic forces can be expressed by a Fourier series, but are dominated by their fundamental components. Although the approach of this study can be generalized, for simplicity, it is assumed that the flapping foils produce forces and moments of the form

$$f_p = F_{10}(S_{t1}, \omega_f) + F_{20}(S_{t2}, \omega_f) + F_{11}(S_{t1}, \omega_f)\cos(\omega_f t + \alpha_1) + F_{12}(S_{t2}, \omega_f)\cos(\omega_f t + \alpha_2)$$
$$m_p = M_{10}(S_{t1}, \omega_f) + M_{20}(S_{t2}, \omega_f) + M_{11}(S_{t1}, \omega_f)\cos(\omega_f t + \alpha_1) + M_{12}(t_{t2}, \omega_f)\cos(\omega_f t + \alpha_2), \tag{3}$$

where S_{ti} is the Strouhal number defined as

$$S_{ti} = \left(\frac{fA_i}{U}\right), \quad i = 1, 2 \tag{4}$$

and is a dimensionless angular frequency parameter, $\omega_f = 2\pi f$ is the frequency of oscillation (rad/s), and A_i is the maximum cross-stream travel of the flap tip. It is important to note that the Strouhal number of each foil is a key control variable that can be altered by the choice of frequency and the tip travel A_i independently, and, thus, one can control the contribution of each foil in force generation for the purpose of control.

For the purpose of control, it is assumed that the two foils are controlled independently and oscillate with the same frequency ω_f, but the maximum travel of each tip A_i is varied at the interval of T_p, the time period of oscillation of foils. A continuous change of A_1 and A_2 is not allowed here since the intention is to develop a periodic force by flapping, although such an imposed mode of oscillation does create a complex control design problem. Note that we are trying to imitate biolocomotion for slow speed maneuvers.

The problem of interest here is to design a control system for the independent control of depth (z) using dorsal fins and stabilize the pitch angle dynamics using flapping foils. This decomposition of the dive plane control problem simplifies the controller design. An adaptive sliding mode control system is designed for large magnitude depth (z), and a discrete adaptive predictive controller is designed for pitch angle regulation separately based on the decoupled rotational dynamics of the pitch angle of the vehicle. A judicious choice of controller design is essential since the dorsal fins are continuously cambered and the parameters of oscillations of the foils can be altered only at the completion of the cycle of flapping at discrete, but uniformly distributed, instants of time.

The system (Eq. (1)) can be written in a vector form as

$$\begin{pmatrix} \dot{z} \\ \dot{w} \\ \dot{q} \\ \dot{\theta} \end{pmatrix} = \begin{bmatrix} -U\sin\theta + w\cos\theta + \dot{z}_f \\ a_1 w + a_2 q + a_3(x_{GB}\cos\theta + z_{GB}\sin\theta) + a_4(w, q) + d_1 \\ a_5 w + a_6 q + a_7(x_{GB}\cos\theta + z_{GB}\sin\theta) + a_8(w, q) + d_2 \\ q \end{bmatrix} + \begin{bmatrix} 0 & 0 & 0 \\ B_{21} & B_{22} & B_{23} \\ B_{31} & B_{32} & B_{33} \\ 0 & 0 & 0 \end{bmatrix} \begin{bmatrix} \delta \\ f_p \\ m_p \end{bmatrix} \tag{5}$$

or

$$\dot{x} = Ax + g(x) + BU_c + Dd \tag{6}$$

where $x = (z, w, q, \theta)^T \in R^4$ is the state vector (T denotes transposition), $U_c = (\delta, f_p, m_p)^T$ is the control vector, $d = (\dot{z}_f, d_1, d_2)^T$, and D, a_i, A, B_{ij} and B are obtained by comparing (6), (7), and (8). The function $g(x)$ is the nonlinear function in (5), and A and D are constant matrices.

Dorsal Fin Control System

In this section, a dorsal fin control system is designed for depth control. Since depth (z) control is of interest, an output controlled variable

$$y_o = z \tag{7}$$

is associated with the system (Eq. (6)). Consider a reference trajectory, $y_r(t)$, generated by a second order command generator

$$\ddot{y}_r + 2\xi_r\omega_r\dot{y}_r + \omega_r^2 y_r = \omega_r^2 z^*, \tag{8}$$

where z^* is the target depth coordinate, $\xi_r > 0$, and $\omega_r > 0$. The parameters ξ_r and ω_r are properly chosen to obtain the desired command trajectories. The objective is to steer the vehicle using the dorsal fins so that $y_o = z(t)$ asymptomatically follows $y_r(t)$. As y_o tends to $y_r(t)$, the vehicle attains the desired depth since y_r converges to z^*.

For the derivation of a controller, an adaptive sliding mode control technique (Slotin and Li, 1991; Utkin, 1978; and Narendra and Annaswamy, 1989) is used and the sliding surface is defined as

$$S = \dot{e} + \lambda e, \tag{9}$$

where $\lambda > 0$ and $e = (y_o - y_r) = z - y_r$ is the tracking error.

Consider the motion during the sliding phase. During the period of sliding, one has $S(t) \equiv 0$, which implies from Eq. (9) that

$$\dot{e} + \lambda e = 0. \tag{10}$$

Thus, during the sliding phase, it follows that $e(t) \to 0$, that is, $z(t) \to z^*$ as $t \to \infty$ and the desired depth control is accomplished.

Now consider the design of a controller so that the trajectory beginning from any initial condition is attracted toward the switching surface. In obtaining a control law, differentiating $S(t)$ along the trajectory of the system (Eq. (6)), and substituting $\dot{\omega}$ from (5), gives

$$\dot{S} = \ddot{e} + \lambda \dot{e} \tag{11}$$

$$= \cos\theta B_{21}[\alpha(x, f_p, m_p, t) + \Delta\alpha(x, d, f_p, m_p, \ddot{z}_f, t) + \eta^T\psi(x) + F_{d1}\cos\omega_o t + F_{d2}\sin\omega_o t + \delta], \tag{12}$$

where $B_{21}^{-1}d_1 = F_{d1}\cos\omega_o t + F_{d2}\sin\omega_o t$. Here α and ψ are known functions, but $\Delta\alpha$, the parameter vector η, the amplitudes F_{d1} and F_{d2}, and B_{21} are unknown. It is assumed that the sign of B_{21} is known and $|\theta| \le \theta_m < \pi/2$. Without loss of generality, it is assumed that $B_{21} > 0$. The known functions α and ψ are computed using the nominal set of values of various parameters of the system.

The camber δ of the dorsal fin is continuously varied to steer any trajectory toward the switching surface. Assuming that the frequency ω_o of the surface wave is known, a control law is now chosen as

$$\delta = -\alpha(x, f_p, m_p, t) - \hat{\eta}^T\psi(x) - \hat{F}_{d1}\cos\omega_o t - \hat{F}_{d2}\sin\omega_o t - \mu S - K\,\mathrm{sgn}\,(S), \tag{13}$$

where $\mu > 0$, $\hat{\eta}$ and $\hat{F}_{di}$ are estimates of η and F_{di}, respectively, and K is a constant gain yet to be determined. Substituting control law Eq. (18) into Eq. (17), gives

$$\dot{S} = \cos\theta B_{21}[\Delta\alpha + \tilde{\eta}^T\psi(x) + \tilde{F}_{d1}\cos\omega_o t + \tilde{F}_{d2}\sin\omega_o t - K\,\mathrm{sgn}\,S - \mu S], \tag{14}$$

where $\tilde{\eta} = \eta - \hat{\eta}$, and $\tilde{F}_{di} = F_{di} - \hat{F}_{di}$.

Now, adaptation laws for $\hat{\eta}$, $\hat{F}_{di}$, and gain K must be chosen so that the surface S becomes attractive to any trajectory of the system. In deriving the adaptation law, consider a Lyapunov function,

$$V_o = ((B_{21}\cos\theta)^{-1}S^2 + \tilde{\eta}^T L_1\tilde{\eta} + \tilde{F}_{d1}^2 L_2 + \tilde{F}_{d2}^2 L_3)/2, \tag{15}$$

where $L_2 > 0$, $L_3 > 0$, and L_1 ($i = 1, 2, 3$) is any positive definitive symmetric matrix which are chosen to provide desirable response characteristics. The derivative of V_o is given by

$$\dot{V}_o = S(\Delta\alpha + \tilde{\eta}^T\psi + \tilde{F}_{d1}\cos\omega_o t + \tilde{F}_{d2}\sin\omega_o t - K\,\mathrm{sgn}\,S) - \mu S^2 + \tilde{\eta}^T L_1\dot{\tilde{\eta}} + L_2\tilde{F}_{d1}\dot{\tilde{F}}_{d1} + L_3\tilde{F}_{d2}\dot{\tilde{F}}_{d2}. \tag{16}$$

The function V_O is a positive definite function of S, $\tilde{\eta}$, $\tilde{F}_{d1}$, $\tilde{F}_{d2}$. In order to ensure that the surface $S = 0$ is attractive, adaptation laws and K are chosen so that $\dot{V}_o$ satisfies $\dot{V}_o \le 0$.

In view of Eq. (16), one chooses the adaptation laws of the form

$$\dot{\hat{\eta}} = -\dot{\tilde{\eta}} = L_1^{-1}\psi S,$$

$$\dot{\hat{F}}_{d1} = -\dot{\tilde{F}}_{d1} = L_2^{-1}S\cos\omega_o t,$$

$$\dot{\hat{F}}_{d2} = -\dot{\tilde{F}}_{d2} = L_3^{-1}S\sin\omega_o t \tag{17}$$

and the gain K is chosen to satisfy

$$K = k_1(\xi, d, f_p, m_p) + \epsilon, \tag{18}$$

where the function k_1 is a bound on the uncertain function satisfying

$$k_1 \ge |\Delta\alpha(x, d, f_p, m_p, \ddot{z}_f, t)|. \tag{19}$$

Substituting adaptation law (17) in Eq. (16) now yields

$$\dot{V}_o \le -\epsilon|S| - \mu S^2 \le 0. \tag{20}$$

Since $\dot{V}_o \le 0$, it follows that S, $\hat{\eta}$, and $\hat{F}_{di}$ are bounded. Furthermore, in view of Eq. (20), one concludes that $S(t) \to 0$, as $t \to \infty$, assuming that θ, q are bounded. This implies that the tracking error $(z - y_r) \to 0$ as $t \to \infty$. This completes the depth control system design.

Assuming that error $y_r(t) \to z^*$, and $\dot{y}_r \to 0$, the control law (Eq. (13)) asymptotically decouples (θ, q) dynamics from the remaining variables. Thus, the residual dynamics of the system essentially describe the rotational pitch motion. This residual dynamics, when the motion is constrained so that the error $y - y_r = 0$, is called the zero-error dynamics (Slotine and Li, 1991). For satisfactory performance in the closed-loop system, the state variables θ and q associated with zero-error dynamics must be bounded. In the next section, control of pitch angle using flapping foils is considered.

Flapping Foil Control of Pitch Dynamics

In this section, control of rotational pitch dynamics (zero error dynamics) is considered. First, a discrete-time linear model for pitch control is obtained.

Discrete-Time Pitch Dynamics. Since the sliding mode controller asymptotically controls z to z^*, the zero error dynamics is obtained from Eq. (1) by setting $\dot{e} = \dot{z} - \dot{y}_r = \dot{z} = 0$. Also, when $e(t) = 0$, $\dot{e}(t) = \dot{z} - \dot{y}_r = \dot{z} = 0$, one has for small θ

$$w = U\theta - \dot{z}_f \tag{21}$$

It is assumed that the two foils oscillate with identical frequency ω_f. The maximum travel A_i of each foil-tip is independently controlled periodically at the interval of T_p ($=2\pi/\omega_f$). This way the Strouhal numbers S_{t1} and S_{t2} of the two foils are independently controlled. The moments, $m_{pi}(S_{ti}, \omega_f)$, and forces, $f_{pi}(S_{ti}, \omega_f)$ ($i = 1, 2$), generated by the flapping foils are nonlinear functions of the Strouhal numbers. Since ω_f is a constant, expanding $f_{pi}(S_{ti})$ and $m_{pi}(S_{ti})$ in the Taylor series about $S_{t1} = S_{t2} = S_t^*$, a constant, and neglecting higher order terms gives

$$B_{33}m_{pi}(S_{ti}) + B_{32}f_{pi} \approx B_{33}\left[\frac{\partial M_{io}(S_t^*)}{\partial St_i} + \frac{\partial M_{1i}(S_t^*)}{\partial S_{ti}}\cos(\omega_f t + \alpha_i)\right]\tilde{S}_{ti} + B_{32}\left[\frac{\partial F_{io}(S_t^*)}{\partial S_{ti}} + \frac{\partial F_{1i}}{\partial S_{ti}}(S_{ti}^*)\cos(\omega_f t + \alpha_i)\right]\underline{\Delta}b_{ii}(t)\tilde{S}_{ti}, \quad i = 1, 2, \tag{22}$$

where $\tilde{S}_{ti} = S_{ti} - S_t^*$.

Next, pitch angle must be regulated to θ^*, a constant. Using Eqs. (16), (17), (20), and (21), the pitch dynamics about (θ^*, $q^* = 0$) obtained from (5) are given by

$$\dot{\tilde{x}} \underline{\Delta} A_p\tilde{x} + b_1[b_{11}\tilde{S}_{t1} + b_{22}\tilde{S}_{t2} + D_2(t)], \tag{23}$$

where $D_2 = d_2 + a_7x_{GB}\cos\theta^* + a_8 + B_{31}\delta + a_5(U\theta^* - \dot{z}_f) + a_7z_{GB}\sin\theta^*$, $b_1 = [1, 0]^T$,

$$\tilde{x} = (q, \tilde{\theta})^T, \ \tilde{\theta} = \theta - \theta^*,$$

and

$$A_p = \begin{bmatrix} a_6 & a_5 U + a_7(z_{GB}\cos\theta^* + x_{GB}\sin\theta^*) \\ 1 & 0 \end{bmatrix}$$

Since the control input $\tilde{S}_{ti}$ is to be implemented as a piecewise constant function changing at the interval T_p, a discrete-time model is obtained from Eq. (23) of the form

$$\tilde{x}(k+1) = A_c\tilde{x}(k) + B_c\tilde{S}_t(k) + D_c(k), \tag{24}$$

where $(k+1)$ denotes $(k+1)T_p$, $\tilde{S}_t(t) = \tilde{S}_t(k) = [\tilde{S}_{t1}(k), \tilde{S}_{t2}(k)]^T$ for $t\epsilon[kT_p, (k+1)T_p)$, and

$$A_c = e^{A_pT_p}$$

$$B_c = \int_{kT_p}^{(k+1)T_p} e^{A_p[(k+1)T_p-\tau)}b_1[b_{11}(\tau), b_{22}(\tau)]d\tau$$

$$D_c(k) = \int_{kT_p}^{(k+1)T_p} e^{A_p[(k+1)T_p-\tau]}b_1D_2(\tau)d\tau. \tag{25}$$

Let $A_c = (a_{cij})$, $B_c = [B_{c1}^T, B_{c2}^T]^T = (b_{cij})$ for $i, j = 1, 2$, and $D_c(k) = (D_{c1}, D_{c2})^T$. Note that B_c is a 2×2 constant matrix since integration in Eq. (35) is performed over one period T_p and $\omega_f = 2\pi/T_p$, but $D_c(k)$ depends on kT_p due to the fact that $\omega_f \neq \omega_o$; that is, the flapping frequency differs from the frequency of the wave.

Autoregressive Moving Average Model. Next, a discrete adaptive predictive control technique is used for pitch control. For this, an expression for the predicted value of $\tilde{\theta}(k)$ is obtained and the advance operator q_a is introduced and defined as $q_az_s(k) = z_s(k+1)$ for any discrete signal $z_s(k)$. Using Eq. (24) gives

$$q_a\tilde{q}(k) = a_{c11}\tilde{q}(k) + a_{c12}\tilde{\theta}(k) + B_{c1}\tilde{S}_t(k) + D_{c1}(k) \tag{26}$$

$$q_a\tilde{\theta}(k) = a_{c21}\tilde{q}(k) + a_{c22}\tilde{\theta}(k) + B_{c2}\tilde{S}_t(k) + D_{c2}(k). \tag{27}$$

Operating (26) and (27) by q_a^{-2} and q_a^{-1}, respectively, and manipulating the resulting equations, it can be shown that (for details, see Singh and Bandyopadhyay, 1997),

$$[1 + (-a_{c11} - a_{c22})q_a^{-1} + (a_{c11}a_{c22} - a_{c21}a_{c12})q_a^{-2}]\tilde{\theta}(k) = q_a^{-1}[B_{c2} + (a_{c21}B_{c1} - a_{c11}B_{c2})q_a^{-1}]\tilde{S}_t(k) + q_a^{-1}[D_{c2}(k) + a_{c21}q_a^{-1}D_{c1}(k) - a_{c11}q_a^{-1}D_{c2}(k)] \tag{28}$$

or

$$(1 + a_{f1}q_a^{-1} + a_{f2}q_a^{-2})\tilde{\theta}(k) = q_a^{-1}(B_{f1} + B_{f2}q_a^{-1})\tilde{S}_t(k) + q_a^{-1}a_{fd}(k), \tag{29}$$

where a_{fi}, B_{fi} and a_{fd} are obtained by comparing (28) and (29).

The discrete-time model of Eq. (29) is called an autoregressive moving average (ARMA) model. The ARMA model can be expressed in an alternative predictor form as

$$\tilde{\theta}(k+1) = (-a_{f1} - a_{f2}q_a^{-1})\tilde{\theta}(k) + (B_{f1} + B_{f2}q_a^{-1})\tilde{S}_t(k) + a_{fd}(k). \tag{30}$$

This is a useful representation of the pitch dynamics. It is assumed that the parameters a_{fi}, B_{fi}, and the signal $a_{fd}(k)$ are unknown. For the regulation of $\theta(k)$, one can design predictive control laws if the estimates of the unknown parameters and $a_{fd}(k)$ are known.

For the derivation of a control law, it is assumed that

$$a_{fd}(k+1) \approx a_{fd}(k). \tag{31}$$

Note that if the wave frequency ω_o is equal to the frequency of flapping and if either δ is small or $B_{31} \approx 0$, then $a_{fd}(k+1) = a_{fd}(k)$ for all k. In practice, it has been found that the predictive control technique works well even when parameters vary slowly and the condition of Eq. (31) is violated.

Under the assumption of Eq. (31), subtracting $q_a^{-1}\tilde{\theta}(k+1)$ from (30) gives

$$\tilde{\theta}(k+1) = [-a_{f1} + (a_{f1} - a_{f2})q_a^{-1} + a_{f2}q_a^{-2}]\tilde{\theta}(k) + [B_{f1} + (B_{f2} - B_{f1})q_a^{-1} - B_{f2}q_a^{-2}]\tilde{S}_t(k)\Delta\upsilon(q^{-1})\tilde{\theta}(k) + \beta(q^{-1})\tilde{S}_t(k), \tag{32}$$

where

$$\upsilon(q_a^{-1}) = \upsilon_0 + \upsilon_1q_a^{-1} + \upsilon_2q_a^{-2},$$
$$\beta(q_a^{-1}) = \beta_0 + q_a^{-1}\beta'(q_a^{-1}),$$
$$\beta'(q_a^{-1}) = \beta_1 + \beta_2q_a^{-1}. \tag{33}$$

The coefficients β_i and υ_i are obtained from (32).

Adaptive Pitch Angle Control. Assuming that the parameters of Eq. (32) are known, now a weighted one-step ahead pitch control law is obtained. For this a suitable performance index of the form

$$J(k+1) = \tfrac{1}{2}[\tilde{\theta}(k+1) - \theta_r^*(k+1)]^2 + \tfrac{1}{2}\lambda_d\|S_t(k)\|^2 \tag{34}$$

is chosen, where $\lambda_d > 0$ and $\theta_r^*(k)$ is a suitable reference trajectory to be followed by $\tilde{\theta}(k)$. Note if $\theta_r^*(k) \to 0$, then $\theta(k) \to \theta^*$. By the choice of a suitable value of λ_d, a compromise between the rate of convergence $\tilde{\theta}(k+1)$ to $\theta^*(k+1)$ and the amount of control effort expended is achieved.

Substituting $\theta(k+1)$ from (32) in (34), for minimizing J differentiating with respect to $S_t(k)$, and solving gives

$$\tilde{S}_t(k) = (\lambda_dI + \beta_o^T\beta_o)^{-1}\beta_o^T[-\upsilon(q_a^{-1})\tilde{\theta}(k) - \beta'(q_a^{-1})\tilde{S}_t(k-1) + \theta_r^*(k+1)] \tag{35}$$

Notice that the Strouhal number at the instant kT_p depends on the present and past values of θ and the past values of input S_t, $\tilde{S}_t$.

Since $\tilde{S}_{ti}(k) \in [0, \tilde{S}_{tim}]$ where $\tilde{S}_{tim}$ is the same maximum allowed value of $\tilde{S}_{ti}$, control input $\tilde{S}_{ti}(k)$ given in (35) must be set to the lower or upper limits whenever the magnitude exceeds the prescribed limits.

Parameter Estimation. For synthesizing the control law, the parameters in Eq. (32) must be known. A practical solution to this problem is to obtain an estimate of these unknown parameters using an appropriate parameter identification technique. There are several kinds of algorithms based on the projection and the least square methods that can be used to obtain the estimates of these unknown parameters β_o, υ_i, and β_i in Eq. (32). Equation (32) can be written as

$$\tilde{\theta}(k+1) = \phi^T(k)\rho_o, \tag{36}$$

where

$$\phi^T(k) = [(1q_a^{-1}q_a^{-2})\tilde{\theta}(k), (1q_a^{-1}q_a^{-2})S_t^T(k)]$$
$$\rho_o^T = [(\upsilon_o, \upsilon_1, \upsilon_2), \beta_o, \beta_1, \beta_2]$$
$$(1, q_a^{-1}, q_a^{-2})S_t^T = (S_t^T, q_a^{-1}S_t^2, q_a^{-2}S_t^T)$$

Using a simple projection algorithm described in Goodwin and Sin (1984) for parameter estimation, the estimate $\hat{\rho}_o$ of ρ_o is obtained using an update law given by

$$\hat{\rho}_o(k) = \hat{\rho}_o(k-1) + \frac{a(k)\phi(k-1)}{c_1 + \phi^T(k-1)\phi(k-1)}[\tilde{\theta}(k) - \phi^T(k-1)\hat{\rho}_o(k-1)] \quad 0 < a(k) < 2,\ c_1 > 0 \tag{37}$$

These parameters are used in (35) for synthesis.

Now the adaptation law for adjusting the maximum travel of the tips of the two foils is easily computed using the definition of the Strouhal number and required adaptation scheme is given by

$$A_i(k+1) = \left[\frac{US_{ti}(k)}{(\omega_f/2\pi)} \right], \quad i = 1, 2, \tag{38}$$

where $S_{ti}(k) = \tilde{S}_{ti}(k) + S_i^*$.

The complete closed-loop system is shown in Fig. 2.

Dorsal Fin Control With Inactive Caudal Fins. In the previous sections, control systems using both the dorsal and caudal fins have been presented. A question of interest arises: Is it possible to maneuver the vehicle using only the dorsal fins? We examine this question in this section. It turns out that the vehicle model under consideration is non-minimum phase (i.e., the transfer function has unstable zero). As such, the sliding mode dorsal fin control law (Eq. (13)) derived in the previous section, cannot accomplish depth control with internal stability in the system and a new sliding mode dorsal fin control law must be derived.

When the caudal fins are inactive, $f_p = m_p = 0$, and (6) simplifies as

$$\dot{x} = Ax + g(x) + b\delta + Dd, \tag{39}$$

where b denotes the first column of B in (6). The system's transfer function with $g = 0$, $d = 0$, relating z and δ is

$$\bar{z}(s)/\bar{\delta}(s) = H(s) = C(sI - A)^{-1}b, \tag{40}$$

where $C = [1, 0, 0, 0]^T$, s is the Laplace variable, and $\bar{z}$, $\bar{\delta}$ denote the Laplace transforms. For the model (39), $H(s)$ is of the form

$$H(s) = k_p(s - \mu_1)(s + \mu_2)d_p^{-1}(s), \tag{41}$$

where $d_p(s) = s^4 + m_3s^3 + m_2s^2 + m_1s$, and $\mu_i > 0$. Thus, $s = \mu_1$ is an unstable zero and $H(s)$ is nonminimum phase.

For the derivation of a control system with internal stability, an approximate output variable z_a is derived such that

$$\begin{aligned} \bar{z}_a(s)/\bar{\delta}(s) = H_a(s) &= \tilde{C}(sI - A)^{-1}b \\ &= -\mu_1 k_p(s + \mu_2)d_p^{-1}(s). \end{aligned} \tag{42}$$

Following Chockalingam (1998), it can be shown that $\tilde{C}$ is given by

$$\begin{aligned} \tilde{C} = -\mu_1 k_p[0, 0, -1, -\mu_2] \\ \times [b, Ab, A^2b, m_3A^2b] + A^3b]^{-1}. \end{aligned} \tag{43}$$

Note that $H_a(s)$ does not have the unstable zero of $H(s)$.

Now a new controlled output variable can be defined as

$$z_a = \tilde{C}x \tag{44}$$

associated with the nonlinear system (39). For $d = 0$, $g(x) = 0$, in view of (40), (41), and (42), it follows that

$$\bar{z}(s) = -\frac{1}{\mu_1}(s - \mu_1) - \bar{z}_a(s), \tag{45}$$

which implies that

$$z(t) = z_a(t) - \frac{1}{\mu_1}\dot{z}_a(t) \tag{46}$$

From (46), it follows that if $z_a(t) \to z^*$, a desired depth, and $\dot{z}_a(t) \to 0$, then $z(t) \to z^*$, and the target depth is attained.

Now a control law is derived to control the new output variable z_a. The Lie derivatives of a function $a(x)$ with respect to the vector field $f(x) \triangleq Ax + g(x)$ are defined as

$$\begin{aligned} L_f(\alpha)(x) &= \frac{\partial \alpha}{\partial x} f(x) \\ L_f^j(\alpha)(x) &= L_f(L_f^{j-1}(\alpha))(x) \\ L_bL_f^k(\alpha)(x) &= \frac{\partial L_f^k(\alpha)}{\partial x} b. \end{aligned} \tag{47}$$

Define

$$L_DL_f^k(\alpha)(x) = \frac{\partial L_f^k(\alpha)}{\partial x} D. \tag{48}$$

Define

$$\begin{bmatrix} \xi_1 \\ \xi_2 \\ \xi_3 \end{bmatrix} = \begin{bmatrix} \tilde{C}x \\ L_f(\tilde{C}x)(x) \\ L_f^2(\tilde{C}x)(x) \end{bmatrix} \tag{49}$$

where $f(x) = Ax + g(x)$. Differentiating ξ_i along the solution of (39) gives

$$\begin{aligned} \frac{d}{dt}\begin{pmatrix} \xi_1 \\ \xi_2 \\ \xi_3 \end{pmatrix} = \begin{bmatrix} \xi_2 \\ \xi_3 \\ a^*(x) + b^*(x)\delta \end{bmatrix} + \begin{bmatrix} \psi_1 \\ \psi_2(x) \\ \psi_3(x) \end{bmatrix} d \\ + \begin{bmatrix} 0 \\ \psi_u(x) \\ 0 \end{bmatrix} d, \end{aligned} \tag{50}$$

where

$$\begin{aligned} \psi_1 = \tilde{C}D,\ \psi = [\psi_1, \psi_2, \psi_3]^T \\ a^* = L_f^3(\tilde{C}x)(x) \\ b^* = L_bL_f^2(\tilde{C}x)(x) \\ \psi_u = L_bL_f(\tilde{C}x)(x) \\ \psi = [\psi_1, L_DL_f(\phi_1)(x), L_DL_f^2(\phi_1)(x)]^T. \end{aligned}$$

For the derivation of control law, small values of ξ, η, δ, and d, functions ψd and $\psi_u\delta$ can be neglected to obtain an approximate representation of the nonlinear system as

$$\frac{d}{dt}\begin{bmatrix} \xi_1 \\ \xi_2 \\ \xi_3 \end{bmatrix} = \begin{bmatrix} \xi_2 \\ \xi_3 \\ a^*(x) + b^*(x)\delta \end{bmatrix} \tag{51}$$

Define $\tilde{\xi}_i = \xi_i - y_r^{(i-1)}$, $i = 1, 2, 3$, where $y_r^{(k)}$, is the kth derivative of the reference depth trajectory.

The sliding surface $S = 0$ is defined as

$$S = \tilde{\xi}_3 + \lambda_2\tilde{\xi}_2 + \lambda_1\tilde{\xi}_1 + \lambda_0\int_0^t \tilde{\xi}_1 dt, \tag{52}$$

which in view of (51) can be written as

$$S = \ddot{\tilde{\xi}}_1 + \lambda_2\dot{\tilde{\xi}}_1 + \lambda_1\tilde{\xi}_1 + \lambda_0\int_0^t \tilde{\xi}_1 dt. \tag{53}$$

The parameters λ_i are chosen such that the polynomial

$$\Pi(s) = s^3 + \lambda_2s^2 + \lambda_1s + \lambda_0 \tag{54}$$

is stable. Differentiating S and using (51) gives

$$\dot{S} = \lambda_2\ddot{\tilde{\xi}}_1 + \lambda_1\dot{\tilde{\xi}}_1 + \lambda_0\tilde{\xi}_1 + a^*(x) + b^*(x)\delta - y_r^{(3)}. \tag{55}$$

In view of (55) the sliding mode dorsal fin control law is given by

$$\delta = (b^*(x))^{-1}[-a^*(x) + y_r^{(3)} - \lambda_2(\xi_3 - \ddot{y}_r) - \lambda_1(\xi_2 - \dot{y}_r) - \lambda_0(\xi_1 - y_r) - k_1 S - k_2 \operatorname{sgn}(S)]. \quad (56)$$

Substituting (56) in (55) gives

$$\dot{S} = -k_1 S - k_2 \operatorname{sgn}(S), \quad (57)$$

which implies that $S(t) \to 0$ and, therefore, according to (53), $\tilde{\xi}_1 \to 0$ as $t \to \infty$, since $\Pi(s)$ is Hurwitz. In the closed-loop systems (51) and (56), for $y_r = z^*$, a constant, $(z_a(t), \dot{z}_a(t)) \to (z^*, 0)$ as $t \to \infty$ and from (46) it follows that $z(t) \to z^*$. As $z(t) \to z^*$, the pitch angle also converges to zero since the transfer function H_a is minimum phase.

For the system (50), it can be proven that for small perturbations in x about the origin and small y_r and disturbance input d, with a proper choice of k_r, the trajectory error remains bounded (Chockalingam, 1998).

Simulation Results. In this section, results of digital simulation are presented. Although a combined dorsal and caudal fin control law has been derived, for simplicity in simulation, numerical results for the system (1) only with the dorsal fin control system (56) is presented and it is assumed that the caudal fins are inactive. The parameters used for simulation are given in the Appendix. For the nominal parameters, the transfer function has two zeros such that $\mu_1 = 4.5325$ and $\mu_2 = 11.3806$. Since the transfer function is nonminimum phase, the row vector $\tilde{C}$ is computed using (43) to yield

$$\tilde{C} = [-8.586e-05, -0.0708, -0.8015, 1.009].$$

The reference trajectory is generated by the fourth-order system given by

$$(s + \lambda_c)^4 y_r - \lambda_c^4 z^* = 0,$$

where z^* is the target depth. The sliding mode parameters are $\lambda_2 = 17$, $\lambda_1 = 64$, $\lambda_0 = 20$. In order to avoid control chattering, sgn (S) was replaced by set (S/ϵ) with $\epsilon = 0.01$.

Define the tracking error for the depth variable $z_e = z - y_r$. Let z_{em}, $\tilde{\xi}_{1m}$, and δ_m be the maximum magnitudes of z_e, $\tilde{\xi}_1$, and camber δ, respectively. In the figures, $\tilde{\xi}_1 = z_a - y_r = \xi_i - y_r$ is denoted by e and u denotes δ.

A. Sliding Mode Dive Plane Control: Nominal System. The complete nominal closed-loop systems (1) and (56), with $f_p = m_p = d = 0$, were simulated. The λ_c of the command generator was chosen to be 0.45. The initial conditions were assumed to be $x(0) = 0$, $y_r^{(k)} = 0$, $k = 0, 1, 2, 3$. A command trajectory was generated for controlling the vehicle to a target depth $z^* = 1m$. The sliding mode gains $k_1 = 1$ and $k_2 = 0.0101$ are chosen. The responses are shown in Fig. 3. We observe smooth control of the vehicle in about 18 seconds. Interestingly, even though the modified output is used for controller design, the depth of the vehicle was controlled smoothly. Apparently, the neglected higher order term $(\psi_u \delta)$ in the design of the sliding mode controller has minor effect on the responses. The maximum depth error and the output errors are $z_{em} = 2.5$ cm and $\xi_{1m} = 2E - 6m$. In steady-state, the pitch angle settles to its equilibrium value zero and the vehicle attains the desired depth. The maximum pitch angle deviation was found to be 0.03°. The maximum camber is $\delta_m = 26.3$ mm. The steady-state values of the heave velocity and the pitch rate were also zero.

It is pointed out that the control magnitude can be reduced by choosing slower command trajectories y_r for the depth control. Simulation was done by setting $\lambda_c = 0.3$ in the command generator. In this case, the maximum control magnitude was reduce to 8 mm, and smooth control was accomplished, but the response time increased to the order of 30 s.

Figure 4 shows the response for a $4m$ ($z^* = 4$) command for a choice of $\lambda_c = 0.3$. This gave a response time of the order of 30 s. The maximum tracking errors are $z_{em} = 6$ cm and $\tilde{\xi}_{1m} = 4E - 5m$. In steady state, the pitch angle settles to its equilibrium value of zero and the tracking errors $\tilde{\xi}_1$ and z_e were found to be zero. The maximum pitch angle deviation was found to be 0.08°. The maximum camber was $\delta_m = 32.3$ mm.

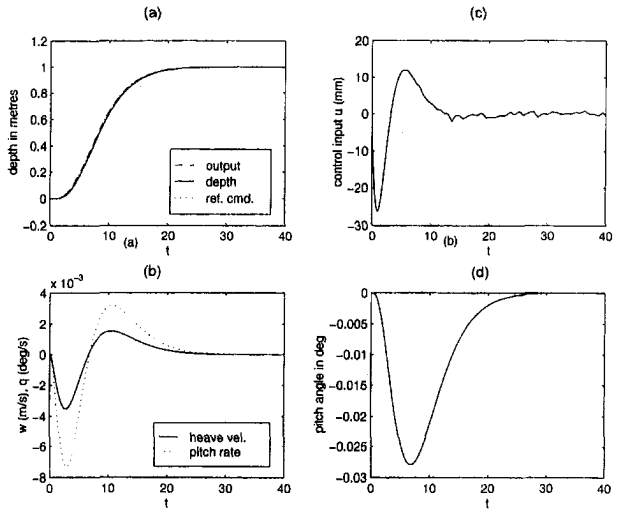

Fig. 3 Dorsal fin control: nominal parameters. (*a*) Output z_a, depth z, and reference command y_r; (*b*) heave velocity and pitch rate; (*c*) camber $\delta = u$; (*d*) pitch angle.

B. Sliding Mode Dive Plane Control: Off-Nominal Parameters. In order to examine robustness of control system, the closed-loop system was simulated with variation of ±25% in the hydrodynamic parameters. The remaining feedback parameters and initial conditions of Fig. 3 were retained. Selected response for +25% parameter perturbations is shown in Fig. 5. We observe smooth control of the vehicle. The steady-state error $\tilde{\xi}_1$ was zero. The pitch angle tends to 0° asympototically. The maximum values are $z_{em} = 2$ cm, $\tilde{\xi}_{1m} = 3E - 4m$, and $\delta_m = 16$ mm. Smaller control input is required in this case since control effectiveness matrix b has increased by an amount of 25%.

Simulation was also done with −25% parameter uncertainty. In this case also, smooth depth control was accomplished and the steady-state error $\tilde{\xi}_1$ was found to be zero. Unlike Fig. 5, larger

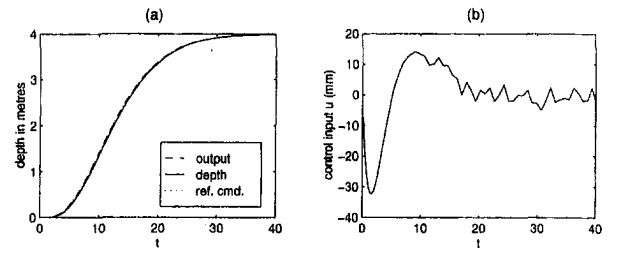

Fig. 4 Dorsal fin control: large command. (*a*) Output z_a, depth z, reference command; (*b*) camber $\delta = u$.

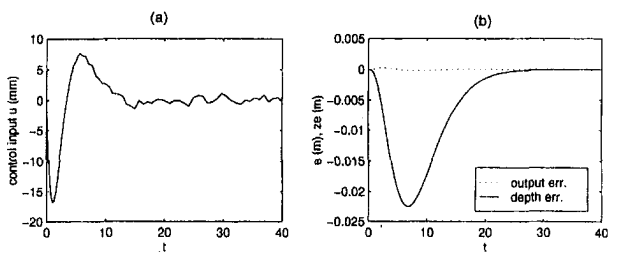

Fig. 5 Dorsal fin control: off-nominal parameters. (*a*) Camber $\delta = u$; (*b*) output error $e = z_a - y_r = \xi_1$ and depth error $z_e = z - y_r$.

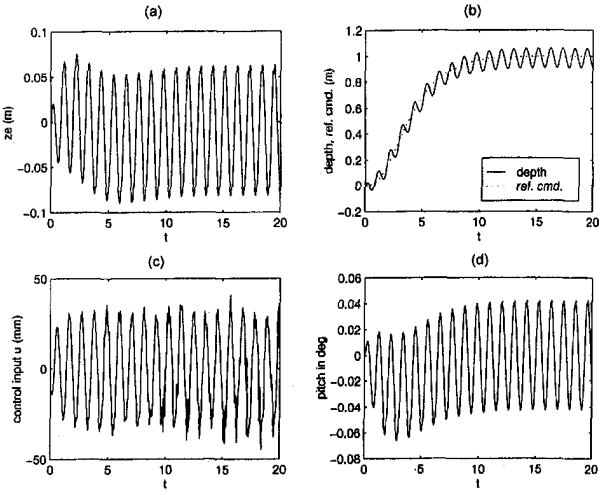

Fig. 6 Dorsal fin control: sinusoidal disturbance. (*a*) Depth error $z_e = z - y_r$; (*b*) depth z and reference command y_r; (*c*) camber $\delta = u$; (*d*) pitch angle.

control is needed for controlling depth since the value of b has decreased. The maximum values are $z_{em} = 5$ mm, $\xi_{1m} = 4$ mm, and $\delta_m = 35$ mm. Since the responses are somewhat similar to those given in Fig. 5 for positive parameter variation, these are not shown.

C. Sliding Mode Dive Plane Control: Sinusoidal Disturbance. Simulation was also done for the depth maneuvering in the presence of sinusoidal disturbance. It was assumed that $f_d = \exp(-0.1z)(0.3075)\ \sin\ (5.817t - \pi)$, $m_d = 0.3512\ \exp(-0.1z)\ \sin\ (5.817t + 70°)$ and $\dot{z}_f = 0.03\ \sin\ (5.817t)$. The frequency and phase angles of the disturbance are close to the values described in Bandyopadhyay et al. (1998). The feedback gains were set as $k_1 = 2$ and $k_2 = 0.01$. Responses for a target depth of $z^* = 1m$ are shown in Fig. 6. The maximum tracking errors were $\xi_{1m} = 7.6$ mm and $z_{em} = 23$ mm. The steady-state oscillation in the depth response is 8 mm. The steady-state oscillation in the pitch was almost negligible. The maximum deviation in the pitch was about 0.02°. The maximum value of the camber was $\delta_m = 31$ mm. It is pointed out that larger gains k_1 and k_2 can be used to attenuate the effect of disturbances of higher amplitudes. But this will require larger camber of the dorsal fins.

Conclusions

A theoretical study for the dive plane control system design for biologically inspired maneuvering of low speed, small undersea vehicles using dorsal and caudal fin-like control surfaces was considered. A hydrodynamic control scheme is developed so that the vehicle tracks a precise depth versus time trajectory. Normal force produced by the dorsal fin was used to control the depth of the vehicle and two flapping foils were used for the pitch angle control. An adaptive sliding mode control law was derived for the reference depth trajectory tracking. For the design of this control, a nonlinear vehicle model was considered for which the system parameters were assumed to be unknown, and it was assumed that sinusoidal disturbance force and moment are acting on the vehicle caused by surface waves. In the closed-loop system, including the sliding mode controller, depth control was accomplished and rotational pitch dynamics were asymptotically decoupled.

For the decoupled pitch dynamics, assuming that the pitch angle perturbations were small, a linear deterministic autoregressive model was derived. For the pitch angle control, the Strouhal numbers were chosen as key input variables. The Strouhal numbers of the two foils were periodically changed (at intervals of the time period of oscillations of the foils by altering the maximum tip travel). Both foils were oscillating at the same frequency. Using projection algorithms, the parameters of the pitch dynamics were identified. These estimated parameters were used to design an adaptive predictive control system for the regulation of the pitch angle. Thus, in the complete closed-loop system, including the adaptive sliding mode and adaptive predictive controllers, dive plane control of the underwater vehicle can be accomplished in the presence of large parameter uncertainty and sea surface waves. A dorsal fin control law was also designed for the control of the vehicle without utilizing caudal fins. Simulation results were presented which showed that depth control and pitch angle regulation can be accomplished by using only dorsal fins.

Acknowledgment

This work was sponsored by ONR (Dr. T. McMullen and Mr. James Fein) and NUWC IR (Dr. S. Dickinson). The support is gratefully acknowledged. This study was carried out while S. Singh served as an ONR Distinguished Faculty Fellow at NUWC Division Newport.

References

Azuma, A., 1992, *The Bio-Kinetics of Flying and Swimming,* Springer-Verlag, New York.

Bainbridge, R., 1963, "The Speed of Swimming of Fish as Related to Size and the Frequency and Amplitude of the Tail Beat," *Journal of Experimental Biology,* Vol. 35, pp. 109–133.

Bandyopadhyay, P. R., 1996, "A Simplified Momentum Model of a Maneuvering Device for Small Underwater Vehicles," NUWC-NPT Technical Report 10,552, Naval Undersea Warfare Center Division, Newport, RI.

Bandyopadhyay, P. R., Nedderman, W. H., Castano, J. M., and Donnelly, M., 1996, "A Small Maneuvering Device for Energetic Environment," NUWC-NPT Video, Naval Undersea Warfare Center Division, Newport, RI.

Bandyopadhyay, P. R., Castano, J. M., Rice, J. Q., Philips, R. B., Nedderman, W. H., and Macy, W. K., 1997, "Low-Speed Maneuvering Hydrodynamics of Fish and Small Underwater Vehicles," ASME JOURNAL OF FLUIDS ENGINEERING, Vol. 119, 1997, pp. 136–144.

Bandyopadhyay, P. R., and Donnelly, M. J., 1997, "The Swimming Hydrodynamics of a Pair of Flapping Foils Attached to a Rigid Body," *Proceedings of the AGARD Workshop on High Speed Body Motion in Water,* Kiev, Ukraine, Sept. 1–3, AGARD Report 827 (Feb., 1998) pp. 1.1–1.17.

Bandyopadhyay, P. R., Nedderman, W. H., and Dick, J., 1999, "Biologically-Inspired Bodies Under Surface Waves. Part 1: Load Measurements," ASME JOURNAL OF FLUIDS ENGINEERING, Vol. 121, published in this issue pp. 469–478.

Chockalingam, F., 1988, "Feedback Linearization of Nominimum Phase Systems and Control of Aeroelastic Systems and Undersea Vehicles," MS thesis, ECE Dept., Univ. Nevada, Las Vegas, April.

Chopra, M. G., 1977, "Hydromechanics of Lunate Tail Swimming Propulsion," *Journal of Fluid Mechanics,* Vol. 7, pp. 46–49.

Goodwin, G., and Sin, K. S., 1984, *Adaptive Filtering Prediction and Control,* Prentice-Hall, Englewood Cliffs, NJ.

Gopalkrishnan, R., Triantafyllou, M. S., Triantafyllou, G. S., and Barrett, D., 1994, "Active Vorticity Control in a Shear Flow Using a Flapping Foil," *Journal of Fluid Mechanics,* Vol. 274, pp. 1–21.

Hall, K. C., and Hall, S. R., 1996, "Minimum Induced Power Requirements for Flapping Flight," *Journal of Fluid Mechanics,* Vol. 323, pp. 285–315.

Healy, A. J., and Lienard, D., 1993, "Multivariable Sliding Mode Control for Autonomous Diving and Steering Unmanned Underwater Vehicle," *IEEE Journal of Oceanic Engineering,* Vol. 18, No. 3, pp. 327–338.

Kailath, T., 1980, *Linear Systems,* Prentice-Hall, Englewood Cliffs, NJ.

Narendra, K. S., and Annaswamy, A. M., 1989, *Stable Adaptive Systems,* Prentice-Hall, Englewood Cliffs, NJ.

Papoulias, F., and Papadimitriou, H., 1995, "Nonlinear Studies of Dynamic Stability of Submarines in Dive Plane," *Journal of Ship Research,* Vol. 39, No. 4, pp. 347–356.

Sastry, S., and Bodson, M., 1989, *Adaptive Control: Stability, Convergence, and Robustness,* Prentice-Hall, Englewood Cliffs, NJ.

Singh, S. N., and Bandyopadhyay, P. R., 1997, "A Theoretical Control Study of the Biologically-Inspired Maneuvering of a Small Vehicle Under a Free Surface Wave," NUWC-NPT Tech Rept. 10816, Aug.

Slotine, J. E., and Li, W., 1991, *Applied Nonlinear Control,* Prentice-Hall, Englewood Cliffs, NJ.

Smith, N. S., Crane, J. W., and Summery, D. C., 1978, "SDV Simulator Hydrodynamic Coefficients," NCSC Rep. TM-231-78, Naval Coastal Systems Center, Panama City, FL, June.

Triantafyllou, M. S., Triantafyllou, G. S., and Gopalakrishnan, R., 1991, "Wake Mechanics for Thrust Generation in Oscillating Foils," *Physics of Fluids,* Vol. 3, No. 12, pp. 2835–2837.

Triantafyllou, G. S., Triantafyllou, M. S., and Grosenbaugh, M. A., 1993, "Optimal Thrust Development in Oscillating Foils With Application to Fish Propulsion," *Journal of Fluids and Structures,* Vol. 7, pp. 205–224.

Utkin, V. I., 1978, *Sliding Modes and Their Application to Variable Structure Systems,* MIR Publication, Moscow.

Wu, T. Y. T., Brokaw, C. J., and Brennen, C., eds., 1975, *Swimming and Flying in Nature,* Vols. 1 and 2, Plenum Press, New York.

APPENDIX

Vehicle parameters:

$$x_{GB} = 0,$$

$$z_{GB} = 0.578802,$$

$$L = 1.282\text{m},$$

$$\rho = 1025.9\text{kgm}^{-3}.$$

Hydrodynamic parameters:

$$U = 3.6\text{m/s},$$

$$M_{\dot{q}} = 0.16E - 3,$$

$$M_{\dot{w}} = -0.825\text{E} - 3,$$

$$M_q = -0.117\text{E} - 2,$$

$$M_w = 0.314E - 2,$$

$$z_\delta = 0.3398,$$

$$z_w = -0.873\text{E} - 2,$$

$$z_{\dot{w}} = -0.569\text{E} - 2,$$

$$z_{\dot{q}} = -0.825\text{E} - 5,$$

$$z_q = -0.238\text{E} - 2..$$